



Delft University of Technology

Topology protection-unprotection transition Example from multiterminal superconducting nanostructures

Huang, Xiao Li; Nazarov, Yuli V.

DOI

[10.1103/PhysRevB.100.085408](https://doi.org/10.1103/PhysRevB.100.085408)

Publication date

2019

Document Version

Final published version

Published in

Physical Review B

Citation (APA)

Huang, X. L., & Nazarov, Y. V. (2019). Topology protection-unprotection transition: Example from multiterminal superconducting nanostructures. *Physical Review B*, 100(8), Article 085408.
<https://doi.org/10.1103/PhysRevB.100.085408>

Important note

To cite this publication, please use the final published version (if applicable).
Please check the document version above.

Copyright

Other than for strictly personal use, it is not permitted to download, forward or distribute the text or part of it, without the consent of the author(s) and/or copyright holder(s), unless the work is under an open content license such as Creative Commons.

Takedown policy

Please contact us and provide details if you believe this document breaches copyrights.
We will remove access to the work immediately and investigate your claim.

Topology protection–unprotection transition: Example from multiterminal superconducting nanostructures

Xiao-Li Huang and Yuli V. Nazarov

Kavli Institute of NanoScience, Delft University of Technology, Lorentzweg 1, NL 2628 CJ, Delft, The Netherlands



(Received 18 August 2017; revised manuscript received 4 June 2018; published 7 August 2019)

We show theoretically that in the superconducting nanostructures the gapped states of different topology are not always protected by separating gapless states. Depending on the structure design parameters, they can be either protected or not, with a protection–unprotection transition separating these two distinct situations. We build up a general theoretical description of the transition vicinity in the spirit of Landau theory. We speculate that similar protection–unprotection transitions may also occur for other realizations of topological protection in condensed matter systems.

DOI: [10.1103/PhysRevB.100.085408](https://doi.org/10.1103/PhysRevB.100.085408)

I. INTRODUCTION

The topological ideas have been a source of inspiration in condensed matter for many decades [1]. In the last decade, there is an outburst of the experimental and theoretical activities related to the topological materials and their unusual transport properties [2–4]. For a material, the topology arises from and is determined by its band structure. One of the remarkable results of the field, that is also of immediate significance, is that there necessarily exist gapless states at the interface between the two insulators of different topology [2]. In the simplest situation, the number of gapless modes at the boundary of different phases is given by the proper difference in their integer-valued topological invariants, as it is the case for quantum Hall states that differ in their Chern number. There is also an intuitive picture behind this mathematical statement: the insulating gaps in the materials are incompatible and can not be continuously changed from one to another, and this implies that the gap must cease in-between. The existence of such gapless states is said to be due to *topological protection*. The gapless edge and surface states provide the transport signatures of topology that are readily accessible for experimental research [5–7].

Many applications and realizations of various topological ideas in condensed matter physics are related to hybrid superconducting heterostructures. Zero-energy Majorana states have been predicted [8,9] and realized [10,11] in such structures and remain in focus of active research. The Weyl points in the spectrum of Andreev bound states of a four-terminal structure [12] have been predicted along with their robust transport signature of quantized transconductance [13] and associated spin effects [14]. A structure combining the topologies of three different kinds has been considered in [15].

A close analog of topological isolators has been predicted and experimentally investigated in [16]. The authors have studied the superconductivity induced in a normal-metal piece connected to three superconducting terminals. Typically, one expects a proximity gap to develop in the normal metal. It turns out that several topologically distinct gapped phases can occur in the structure; those can be characterized by two

integer topological numbers related to the number of windings of the semiclassical Green’s function [15–17].

The use of the semiclassical Green’s functions in superconducting structures is a well-established approach [18–20]. The semiclassical Green’s functions are defined in coinciding space points and thus depend on a single coordinate only. Generally, the Green’s function at a point \mathbf{r} in the structure is an energy-dependent 2×2 Nambu matrix $g_1\sigma_1 + g_2\sigma_2 + g_3\sigma_3$ parametrized by a unit vector \vec{g} , $\vec{g}^2 = 1$ where g_3 gives the density of states (DOS) at zero energy. Importantly, in a gapped phase at zero energy, $g_3 = 0$, $\vec{g} = (\sin \mu, \cos \mu, 0)$, and the parametrizing variable $\mu(\mathbf{r})$ at a terminal equals to the corresponding superconducting phase ϕ . The topological numbers are defined as

$$2\pi N_{ij} = \oint d\mathbf{r} \cdot \nabla \mu(\mathbf{r}) + \phi_i - \phi_j, \quad (1)$$

where the integration contour goes from the terminal i to the terminal j and eventual jumps of μ along the contour are added upon projection of a jump into $(-\pi, \pi)$ interval [16]. If μ were the phase of the superconducting pair potential Δ , the above relation would be well-known contour integral related to Abrikosov vortices and flux quantization [21]. However, μ is not related to the phase of Δ ; the pairing potential can be even absent in the structure, so that Eq. (1) presented an independent topological number. Such definition of topological numbers implies no periodicity in superconducting phases, while the physical situation is obviously periodic. This is no problem since the shift of all topological numbers with the same integer reproduces the same physical situation.

The topologically distinct phases are realized in different regions of the parameter space spanned by two superconducting phase differences between the terminals. General concept of topological protection implies that these regions are separated by finite strips of *gapless* phase, owing to the different nature of these gapped phases. Although in this case the number of the gapless modes is not possible to introduce, their existence seems to be topologically justified. The gapless

modes have been probed by transport in the extra tunnel junction between the structure and a normal-metal lead [16].

In this paper, we investigate the concept of such topological protection in more detail for a case of a general multiterminal superconducting nanostructure. Surprisingly, the topological protection is not a universal property. We have found that depending on the parameters characterizing the nanostructure design, the protection may cease. In this case, the distinct gapped phases are *not* separated by a gapless strip. The parameter regions where the protection persists/ceases are separated by *protection–unprotection* second-order transitions (PUT).

It is common to describe any second-order transitions with Landau approach [22,23]. We have established that the vicinity of PUT is described by a special Landau action that, in distinction from a common Landau action, is for an energy-dependent order parameter. This parameter stems from the Green's functions in the structure. This peculiarity, as we show, gives rise to *two* order parameters that are nonzero above and below the transition: the gap and the density of states (DOS) at zero energy. This makes the Landau action in use especially suitable for description of the situations where the gapless phase emerges and disappears, that is, for PUT.

The Landau action depends on a handful of parameters and hardly reflects any specifics of superconducting nanostructures. This is manifesting for a common Landau approach that is universal for second-order transitions of any kind. This makes us speculate that this universality also holds for the Landau action proposed in the paper. It contains no detail specific to the nanostructures or superconductivity. So, we suggest that this form is universal and can describe similar PUTs in general topological gapped phases that have nothing to do with the nanostructures and superconductivity, for instance, in solid-state topological insulators.

To avoid any misunderstanding, we shall acknowledge that we do not know any physical mechanism or situation that would enable PUT in other condensed matter systems: however, they may become known in the future. The analogy between edge states in solids where the topological phases are separated in real space and the gapless phases in the superconducting nanostructures that separate the phases in a parameter space may seem far fetched, but in fact relies on the same elementary topological reasoning: Two gapped phases with distinct topological numbers cannot be transformed to each other without breaking the gap, if the transformation is continuous. In solids, special symmetries may be required to protect topological order (see, e.g., [24]): This is not the case of the nanostructures. There are interesting developments of Landau approach related to quantum criticality in symmetry-protected situations [25]: This is not related to the PUT we consider here. Our Landau action corresponds to a zero-dimensional situation, and we treat it here in saddle-point approximation, thus disregarding quantum fluctuations. The investigation of the quantum fluctuations in this setup is a relevant and interesting research topic.

The structure of the paper is as follows. We choose to alternate more descriptive and more technical sections. We start with a concrete example of a system where a series of PUTs can be realized (Sec. II). Further, in Sec. III we generalize the consideration to arbitrary nanostructures using

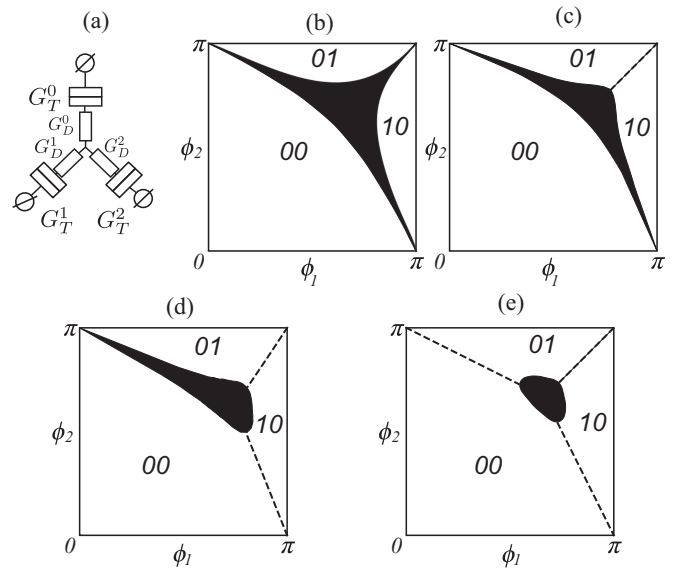


FIG. 1. Protection–unprotection transitions exemplified with a three-terminal circuit that is made from tunnel junctions with conductances G_T^i and diffusive connectors with conductances G_D^i . Three topologically distinct phases N_{00} , N_{10} , N_{01} can occur in this setup, N_{00} being topologically trivial. (a) The topological protection implies that the domains of the three topologically distinct gapped phases in ϕ_1 - ϕ_2 are separated by the gapless state [black in (b)–(e)]. The domain of the gapless state is thin near the special points $(0, \pi)$, $(\pi, 0)$, (π, π) . The protection holds for all three points for sufficiently small diffusive conductances as compared to tunnel ones. Upon increasing the conductances, the protection ceases at special points with three protection–unprotection transitions. Dashed lines indicate unprotected domain boundaries. For calculations, all G_T are taken the same and $G_D^{0,1,2} = 1.5G_T$ (b); $G_D^0 = 10G_T$, $G_D^{1,2} = 1.5G_T$ (c); $G_D^0 = G_D^1 = 10$, $G_D^2 = 1.5$ (d); $G_D^{0,1,2} = 10G_T$ (e).

the semiclassical circuit theory detailed in Sec. IV. We find that the PUTs are manifested in special points of the space of the superconducting phases. In Sec. VI we study in detail the vicinity of a special point, providing the details of the calculation in Sec. VII. In Sec. VIII we concentrate on the vicinity of a PUT, establish the form of the Landau action, and analyze it, providing the detailed derivation in Sec. IX.

II. CONCRETE ILLUSTRATION

Let us give a concrete example of the PUTs with a three-terminal setup that is similar to the experimental system [16]. The setup comprises three tunnel junctions adjacent to the terminals that are connected by diffusive pieces [Fig. 1(a)]. The design parameters are the conductances G_D^i , G_T^i , $i = 0, 1, 2$. We solve for the Green's functions in the structure at zero energy with the standard quantum circuit-theory method [20], the details are given in Sec. V. In Fig. 1 we plot the occurrence regions of each topological gapped phase in ϕ_1 - ϕ_2 plane. Black gives the occurrence region of the gapless phase. In a fully protected situation [Fig. 1(b)] where G_D are small or comparable with G_T , the topological phases are separated from each other by the gapless phase. We observe that the width of the separating region vanishes precisely at special

points, where all phase differences are either 0 or π . Upon decreasing G_D we observe that the topological protection ceases step by step: The region of the gapless phase gets torn off one [Fig. 1(c)], two [Fig. 1(d)], and three [Fig. 1(e)] special points. The tearing off a point corresponds to a PUT. In an unprotected situation, the topological phases are separated by dashed lines where the gap is finite and the phase drop at a tunnel junction equals $\pm\pi$. In fact, similar PUTs have been seen in numerical simulations for a less realistic junction models [26] but have received neither attention nor theoretical explanation.

III. GENERAL SITUATION

After this concrete example, we turn to the general situation: How does a PUT occur for a general N -terminal junction structure? An arbitrary general design can be described by means of finite-element quantum circuit theory where the structure is subdivided into nodes and connectors [20] (see Sec. IV for details). The Green's functions in the nodes are obtained from the minimization of the action

$$S = \sum_c S_c (\vec{g}_{c1} \cdot \vec{g}_{c2}), \quad (2)$$

where the summation is over the connectors, and $c1, c2$ denote the ends of a connector, that can be either nodes or terminals. We resort to imaginary energy (ε) description where the vector \vec{g} is conveniently real at any energy. The Green's functions in N terminals are fixed to $\vec{g} = (\varepsilon, \sin \phi, \cos \phi) / \sqrt{1 + \varepsilon^2}$, $\varepsilon \equiv \varepsilon / \Delta$ being the energy in units of the superconducting energy gap Δ in the terminals. It is instructive to visualize the Green's functions in the structure as nodes of a network made of elastic strings (connectors) stretched over the upper hemisphere, S corresponding to elastic energy. The network is pinned in the points corresponding to \vec{g} in the terminals. It is clear that if the pins are at the equator, the network either spans over the equator (gapped phase) or sprawls over the whole hemisphere (gapless phase) (see Fig. 2).

In $(N - 1)$ -dimensional space of independent phases, we find $2^{N-1} - 1$ special points where the phase differences are either 0 or π and where the PUTs may occur. It helps to

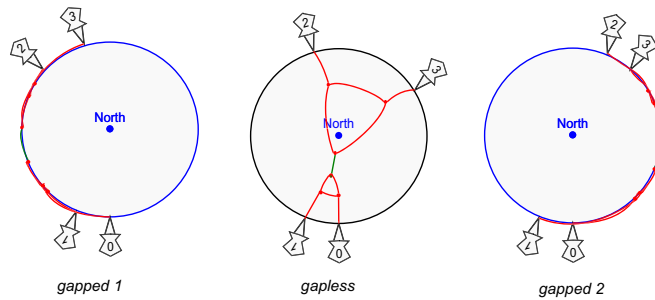


FIG. 2. The Green's functions in an arbitrary superconducting structure can be visualized with a network of elastic strings pinned in the points corresponding to \vec{g} in the terminals. For this example, the circuit encompasses 4 terminals, 6 nodes, and 11 connectors. Depending on the positions of the pins along the equator, the network can either lie at the equator (gapped phase) or rise over the whole hemisphere (gapless phase).

start with a common and rather degenerate case of $N = 2$ where there is only a single superconducting phase difference ϕ , the special point is at $\phi = \pm\pi$, and the gapless phase may exist in this point only. The energy levels in the gap at this point correspond to transmission eigenvalues T_n [27], $E_n = \Delta \sqrt{1 - T_n}$. The protection corresponds to a transmission distribution that spreads until $T \rightarrow 1$, while unprotection corresponds to a distribution that ends at some $T_c < 1$. The PUT thus corresponds to a “localization” transition reported in [28] that for a diffusive-tunnel structure takes place at $G_T = G_D$.

IV. CIRCUIT THEORY

Our approach to multiterminal junction is based on the semiclassical circuit theory [20]. Let us shortly outline it here. In the circuit theory framework, a nanostructure is discretized into terminals, nodes, and connectors between them. A terminal or a node is described by a Green's function G_i . G_i can be geometrically represented as a unit vector \vec{g}_i on a sphere. In Cartesian coordinate system (x, y, z) , the north is chosen to be in z direction. The longitude of \vec{g}_i is the superconducting phase of the corresponding terminal/node, while the z component z_i is equal to $\varepsilon / \sqrt{\varepsilon^2 + \Delta^2}$, where ε is the energy argument of G_i and Δ is the superconducting gap.

A connector positioned between the terminals/nodes i, j can be described with an action $S_{i,j}$ that is a function of G_i and G_j . In general,

$$S = \frac{1}{2} \sum_p \text{Tr} \left\{ \ln \left[1 + \frac{T_p}{4} (G_1 G_2 + G_2 G_1 - 2) \right] \right\}, \quad (3)$$

where T_p is the transmission eigenvalue of that connector. A matrix current $I_{i \rightarrow j}$ through connector between nodes i and j can be computed as $[\frac{\delta S}{\delta G_i}, G_j]$ with the brackets denoting the commutator. This matrix current satisfies Kirchhoff's law at each node. The action can also be written as a function of a parameter ϕ , which, in the geometric representation, is $\arccos(\vec{g}_i \cdot \vec{g}_j)$. The actions for some simple type of connectors are tunneling junction

$$S = -\frac{G_T}{2} \sin^2 \frac{\phi}{2}, \quad (4)$$

diffusive junction

$$S = \frac{G_D}{8} \phi^2, \quad (5)$$

and ballistic junction

$$S = -G_B \ln \cos \frac{\phi}{2}. \quad (6)$$

Here, we used the unit system in which the conductance quantum G_Q is 1. The action of the system is the sum of all connector actions. One can find the ground state of the complete system by minimizing the system action. Equivalently, one can compute the matrix current and apply the Kirchhoff's law.

A conveniently intuitive picture is that of a network of elastic strings (connectors) whose nodes correspond to the \vec{g} and that is stretched over an upper hemisphere being pinned in the points corresponding to the Green's functions in the

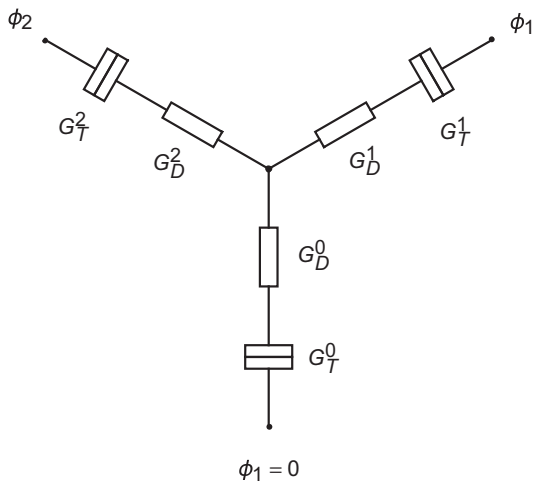


FIG. 3. A three-terminal four-node circuit.

terminals. The action is proportional to elastic energy of the network. At zero ε , the pins are at the equator, and it is clear that the network can either lie at the equator or, being stretched by pins from opposite sides, sprawl over the whole hemisphere (Fig. 2).

V. THREE-TERMINAL STRUCTURE

The three-terminal junction whose phase diagram was presented in Fig. 1 is shown in Fig. 3. The three terminals are all superconducting and gapped. In other words, their corresponding unit vectors \vec{g}_i lie on the equator. Terminal 1 is always kept at phase 0. For comparison with experiments, we have chosen to set ϕ_2 be π minus the actual superconducting phase at terminal 2, so that ϕ_2 is always a positive phase difference between terminals 0 and 2 that lies in the range $(0, \pi)$. Depending on the phases of terminals 1 and 2, as well as the conductance of each of the connectors, the central node can be in gapped or gapless states. Figure 1 shows the phase diagram on (ϕ_1, ϕ_2) plane for different circuit parameters. It is clear there are three special points, where the gapless area is thinnest, and they start to disconnect upon change of circuit parameters. The condition for the transition can be found by determining the phase on the central node ϕ_c on the equator. For example, when $\phi_1 = \phi_2 = \pi$, if $\phi_c \neq \pi$, the node will move on to the north hemisphere upon certain perturbation to ϕ_1 and ϕ_2 , and the gap will close, while the gap will remain open if $\phi_c = \pi$. Simple calculation reveals that the phase transition condition at (π, π) is

$$\frac{G_{D_0}G_{T_0}}{G_{D_0} - G_{T_0}} = \frac{G_{D_1}G_{T_1}}{G_{D_1} + G_{T_1}} + \frac{G_{D_2}G_{T_2}}{G_{D_2} + G_{T_2}}. \quad (7)$$

Similar conditions at the special points $(0, \pi)$ and $(\pi, 0)$ are obtained with exchange of the terminal indices.

The phase boundary between gapped and gapless phases across the whole (ϕ_1, ϕ_2) plane cannot be found in an analytic way, for which we did numerical calculations. Due to the

algorithm used in the program, the calculation could not be done precisely $\epsilon = 0$. We computed the DOS of the central node and set a DOS threshold for to decide whether a point (ϕ_1, ϕ_2) is in the gapped or gapless area. The specific threshold used for Figs. 1(a), 1(b), 1(c), and 1(d) are 0.01, 0.0015, 0.001, and 0.001.

We are also interested in knowing which topological sector the junction is in when gapped. Here, we prefer avoiding general discussion of the definition of distinct sectors. Rather, we illustrate by focusing on the area close to (π, π) . When ϕ_1 and ϕ_2 deviate from π in different directions on the equator, the junction is one topological sector or the other depending on whether ϕ_c sits on the left or right side of π . Using Kirchhoff's law, the boundary between the different topological sectors is found to be a curve that can be parametrized as

$$\phi_1 = \pi - \theta - \arcsin \frac{G_{D_1}}{G_{T_1}} \theta, \quad (8)$$

$$\phi_2 = \pi - \frac{G_{D_1}}{G_{D_2}}\theta - \arcsin \frac{G_{D_1}}{G_{T_2}}\theta. \quad (9)$$

Similar relations for $(0, \pi)$ and $(\pi, 0)$ are obtained by exchange of the terminal indices.

VI. DEEP PROTECTION REGIME

Before concentrating on a PUT, let us understand and describe the vicinity of a special point deep in the protected regime. Let us note that at the special point and at zero energy all the nodes are separated in two groups located at $\vec{g} = (0, \pm 1, 0)$. Owing to this, the solution for Green's functions in this point is degenerate with respect to rotation about the y axis by angle ψ and in each node i can be parametrized as $\vec{g}_i = (\sin \theta_i \cos \psi, \cos \theta_i, \sin \theta_i \sin \psi)$. The visualizing network is thus spanned along a big semicircle defined by points $(0, \pm 1, 0)$ (see Fig. 4). The deviations from the vicinity of the special point both in energy and the phases of the terminals lift the degeneracy and can be casted into the action of the following form (see Sec. VII for the details of the derivation):

$$\mathcal{S}/G = -\chi \cos \psi - \epsilon \sin \psi - r^2 \sin^2 \psi. \quad (10)$$

Here, G is a coefficient of the order of dimensionless structure conductance that is irrelevant for the minimization. Two topological phases corresponding to $\psi = 0, \pi$ are realized in two $(N - 1)$ -dimensional regions that touch each other in the special point. There is a main axis orthogonal to the gapless region surfaces in the special point, and χ stands for the deviation from the special point in the direction of this main axis. The r gives the distance from the special point in all other $N - 2$ directions perpendicular to the main axis. The term with ϵ pulls the Green's functions in 3-direction. With this, we can find the DOS in the nodes of the structure. While the maximum DOS is node specific, $\nu_{m,i} = v_0 \sin \theta_i$, its overall behavior is the same for all nodes:

$$v_i/v_{m,i} = \sqrt{1 - (\chi/2r^2)^2}. \quad (11)$$

The DOS may be regarded as an order parameter in the gapless phase restricted by $|\chi| < \chi_c = 2r^2$. Somewhat

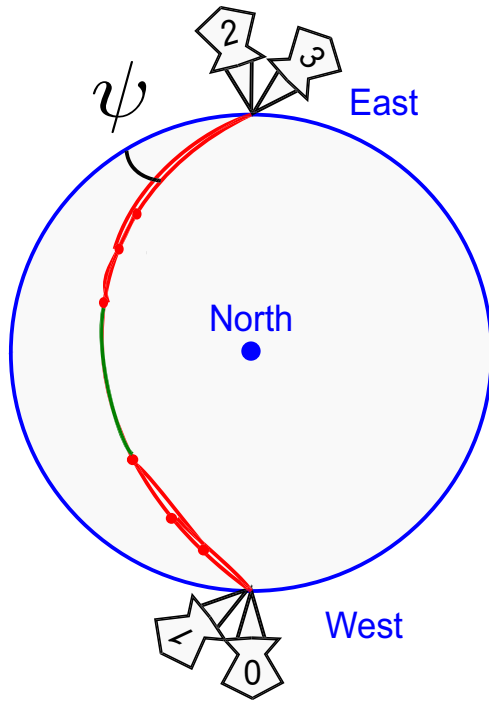


FIG. 4. In a special point, all terminals in one of two positions $(0, \pm 1, 0)$ (west and east poles of the hemisphere). Deep in the protected regime, the network nodes are spanned along one of the big semicircles between east and west poles. Owing to rotational symmetry, the action is the same for any ψ . This degeneracy is lifted by small deviations of the terminal positions.

surprisingly and importantly, the action (10) can be also used to find the gap, a *complementary order parameter* for the gapped phase. Since the gap edge corresponds to a singularity in the Green's function, the gap is found from the conditions of the action minimum and bifurcation $\partial S/\partial\psi = \partial^2 S/\partial\psi^2 = 0$ that is satisfied at imaginary $\epsilon = i\epsilon_g$:

$$\epsilon_g = \chi_c((\chi/\chi_c)^{2/3} - 1)^{3/2}. \quad (12)$$

We illustrate the profiles of the DOS and the gap in Fig. 5.

VII. DEEP IN THE PROTECTED REGIME: DETAILS AND THE DERIVATION

Let us present a derivation of the action (10). Consider a structure with M nodes, denoted by indices $i, j, k \dots$ and N terminals, denoted by indices $a, b, c \dots$. The terminals are close to the east or west poles which are on the equator, while the nodes are sufficiently far away from the poles. In addition to the three-dimensional (3D) Cartesian system (x, y, z) , a spheric polar coordinate system (θ, ψ) will also be used. We define the west and east poles on the equator to be points $(0, 1, 0)$ and $0, -1, 0$. $\theta \in [0, \pi]$ will be the longitude measured from the west pole on the equator, and ψ the azimuth angle with respect to the west-east axis. $\psi = 0$ for the half of equator where $0 < \theta < \pi$. In terms of θ_i and ψ_i , the coordinate of vector \vec{g}_i

$$\vec{g}_i = [-\sin(\theta_i)\cos(\psi_i), \cos(\theta_i), -\sin(\theta_i)\sin(\psi_i)]. \quad (13)$$

Suppose when all the terminals sit at the poles, the equilibrium position of the nodes is (θ_i, ψ_i) , i.e., all the nodes reside on one big circle on the sphere. This is not necessarily the only equilibrium configuration, but is the physically relevant one. Note ψ is a free number as the system has rotational symmetry with respect to west-east axis. Now consider the situation where each terminal deviates from the poles by longitude χ_a , and uniformly above the equator by amount $z = \frac{\epsilon}{\sqrt{\Delta^2 + \epsilon^2}}$. For convenience, let $\epsilon = \epsilon/\Delta$. The new coordinate of the terminals and the nodes is

$$\vec{g}_a = \frac{1}{\sqrt{1 + \epsilon^2}}(-\zeta_a \sin \chi_a, \zeta_a \cos \chi_a, \epsilon). \quad (14)$$

Here, $\zeta_i = \pm 1$, depending on whether the terminal is close to the west pole or east pole. Our aim is to find the new minimum action state of the system. Vary the coordinates of the nodes as

$$\vec{g}_i = [-\sin(\theta_i + \delta\theta_i)\cos(\psi + \delta\psi_i), \cos(\theta_i + \delta\theta_i), -\sin(\theta_i + \delta\theta_i)\sin(\psi + \delta\psi_i)]. \quad (15)$$

To shorten the notations, we introduce two vectors for variations in the unit vector's coordinates:

$$\delta\psi = \begin{pmatrix} \vdots \\ \delta\theta_i, \\ \vdots \\ \delta\psi_i \\ \vdots \end{pmatrix}, \quad \eta = \begin{pmatrix} \vdots \\ \chi_a \\ \vdots \\ \epsilon \\ \vdots \end{pmatrix}. \quad (16)$$

Up to second order in $\delta\psi$ and η , the variation in the action from the original state is

$$\begin{aligned} \delta S = & \frac{\partial S}{\partial \eta_a} \eta_a + \frac{\partial S}{\partial \psi_i} \psi_i + \frac{1}{2} \frac{\partial^2 S}{\partial \eta_a \partial \eta_b} \eta_a \eta_b \\ & + \frac{1}{2} \frac{\partial^2 S}{\partial \eta_a \partial \psi_i} \eta_a \delta\psi_i + \frac{1}{2} \frac{\partial^2 S}{\partial \psi_i \partial \psi_j} \delta\psi_i \delta\psi_j, \end{aligned} \quad (17)$$

where $\frac{\partial S}{\partial \psi_i} \psi_i = 0$ since the derivative is evaluated at the equilibrium. Define matrices A, C and vectors b, d as

$$A_{i,j} = \frac{\partial^2 S}{\partial \psi_i \partial \psi_j}, \quad (18)$$

$$b_i = \frac{\partial^2 S}{\partial \psi_i \partial \eta_j} \eta_j = \frac{\partial^2 S}{\partial \psi_i \partial \chi_a} \chi_a + \frac{\partial^2 S}{\partial \psi_i \partial \epsilon} \epsilon, \quad (19)$$

$$C_{a,b} = \frac{\partial^2 S}{\partial \eta_a \partial \eta_b}, \quad (20)$$

$$d_a = \frac{\partial S}{\partial \eta_a}. \quad (21)$$

The $\delta\psi$ -dependent terms in δS are then

$$\frac{1}{2}(\delta\psi^T A \delta\psi + b^T \delta\psi), \quad (22)$$

the minimum of which is

$$\min \left[\frac{1}{2}(\delta\psi^T A \delta\psi + b^T \delta\psi) \right] = -\frac{1}{8} b^T A^{-1} b. \quad (23)$$

By doing so, we eliminate all $\delta\theta_i$ and $\delta\psi_i$. With χ_a and ϵ fixed, we now have an expression that has only one free parameter ψ .

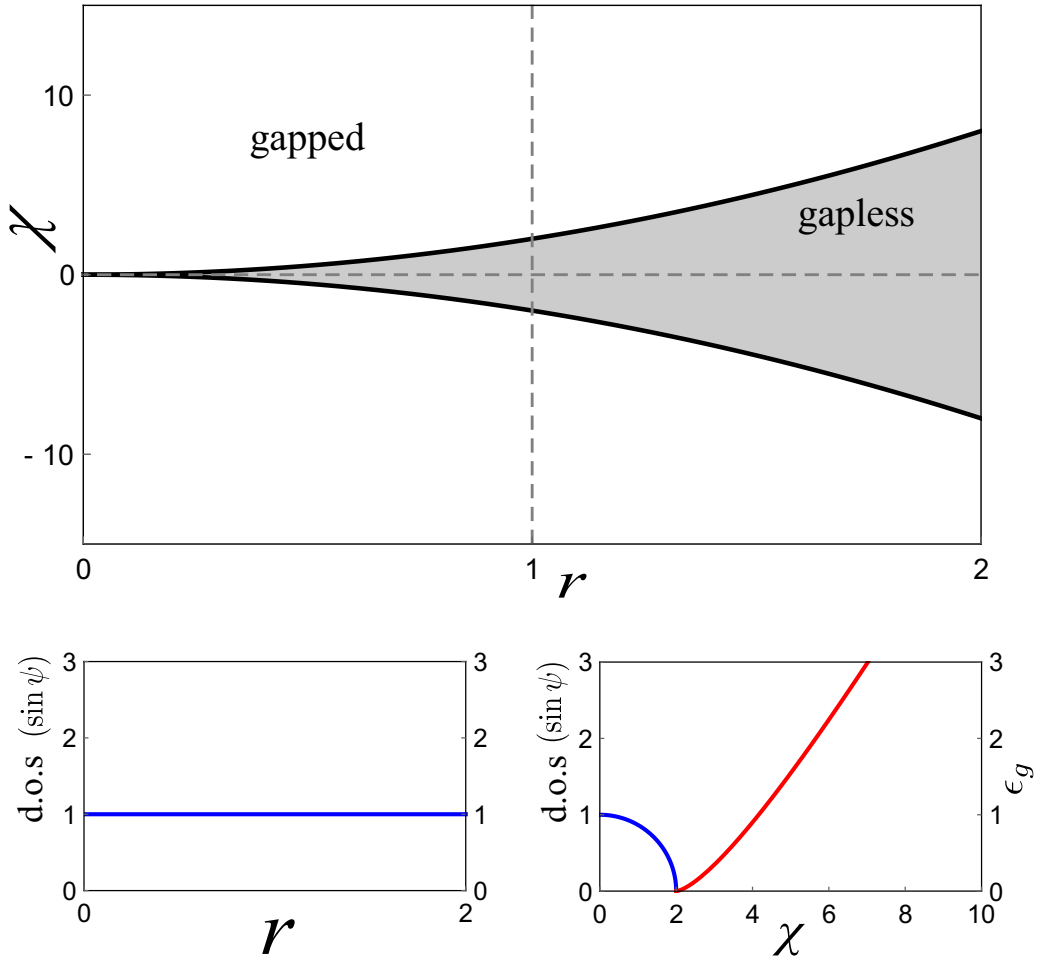


FIG. 5. The vicinity of a special point in the protected regime. Upper part: the domains of gapless and gapped states in the χ - r plane. Lower: the plots of the gap and DOS along the horizontal (left) and the vertical (right) dashed lines in the upper figure.

The equilibrium configuration can be found by minimizing

$$\delta S = -\frac{1}{8}b^T A^{-1}b + \eta^T C\eta + d\eta \quad (24)$$

with respect to ψ . Explicitly,

$$\begin{aligned} & -\frac{1}{8}b^T A^{-1}b + d\eta \\ &= \chi_a \sum_i \frac{\partial S}{\partial p_{i,a}} \sin \theta_i \cos \psi - \epsilon \sum_{i,a} \frac{\partial S}{\partial p_{i,a}} \sin \theta_i \sin \psi \\ & - \frac{1}{8} A_{i,j}^{-1} \left[\left(\frac{\partial^2 S}{\partial p_{i,a}^2} \sin^2 \theta_i - \frac{\partial S}{\partial p_{i,a}} \cos \theta_i \right) \right. \\ & \times (\chi_a \cos \psi - \epsilon \sin \psi) \left. \right] \\ & \times \left[\left(\frac{\partial^2 S}{\partial p_{j,b}^2} \sin^2 \theta_j - \frac{\partial S}{\partial p_{j,b}} \cos \theta_j \right) (\chi_b \cos \psi - \epsilon \sin \psi) \right] \end{aligned} \quad (25)$$

and

$$\begin{aligned} \eta^T C\eta &= \chi_a^2 \left(\frac{\partial^2 S}{\partial p_{i,a}^2} \sin^2 \theta_i \cos^2 \psi + \frac{\partial S}{\partial p_{i,a}} \cos^2 \theta_i \right) \\ & + \chi_a \epsilon \frac{\partial^2 S}{\partial p_{i,a} \partial p_{j,a}} \sin \theta_i \sin \theta_j \sin \psi \cos \psi \\ & + \epsilon^2 \left(\frac{\partial^2 S}{\partial p_{i,a} \partial p_{j,a}} \cos \theta_i \cos \theta_j - \frac{\partial S}{\partial p_{i,a}} \sin \theta_i \sin \psi \right). \end{aligned} \quad (26)$$

Here, we used the notation $p_{i,j} = \vec{g}_i \cdot \vec{g}_j$. Keeping the first-order terms, and terms second order in χ which do not vanish when the first-order terms vanishes, we have

$$\begin{aligned} & -\frac{1}{8}b^T A^{-1}b + d\eta + \eta^T C\eta \\ &= \sum_a \chi_a F_a \cos \psi + \epsilon G \sin \psi + \chi_a \chi_b H_{a,b} \cos 2\psi, \end{aligned} \quad (27)$$

where

$$F_a = \sum_i \frac{\partial S}{\partial p_{i,a}} \sin \theta_i, \quad (28)$$

$$G = \sum_{i,a} \frac{\partial S}{\partial p_{i,a}} \sin \theta_i, \quad (29)$$

$$H_{a,b} = -\frac{1}{16} \sum_{i,j} A_{i,j}^{-1} \left(\frac{\partial^2 S}{\partial p_{i,a}^2} \sin^2 \theta_i - \frac{\partial S}{\partial p_{i,a}} \cos \theta_i \right) \\ \times \left(\frac{\partial^2 S}{\partial p_{j,a}^2} \sin^2 \theta_j - \frac{\partial S}{\partial p_{j,a}} \cos \theta_j \right) + \frac{1}{2} \delta_{a,b} \frac{\partial^2 S}{\partial p_{i,a}^2} \sin^2 \theta_i. \quad (30)$$

Let $\chi' = -\sum_a \chi_a F_a / G$, and $r = \sqrt{2\chi_a \chi_b H_{a,b} / G}$, and we have a dimensionless effective action

$$S/G = -\chi \cos \psi - \epsilon \sin \psi - r^2 \sin^2 \psi. \quad (31)$$

Next, we analyze the system at zero energy based on this action. First, we find the angle ψ_0 that minimizes the action:

$$\psi_0 = \begin{cases} 0, & \chi > 2r^2 \\ \arccos \frac{\chi}{2r^2}, & \chi < 2r^2. \end{cases} \quad (32)$$

Clearly, the junction is gapless when $\chi < 2r^2$, and gapped when $\chi > 2r^2$. $\chi = 2r^2$ is the phase boundary. In the gapless state, the ratio between the density of states for each node and the maximum DOS of that node is simply

$$\nu/\nu_m = \sin \psi_0 = \sqrt{1 - \frac{\chi^2}{4r^4}}. \quad (33)$$

For the gap in gapped state, we put ϵ back to the action and solve the equations

$$\frac{\partial S}{\partial \psi} = \chi \sin \psi - \epsilon \cos \psi - 2r^2 \sin \psi \cos \psi = 0, \quad (34)$$

$$\frac{\partial^2 S}{\partial \psi^2} = \chi \cos \psi + \epsilon \sin \psi - 2r^2 (\cos^2 - \sin^2) \psi = 0 \quad (35)$$

for a purely imaginary solution, the result is

$$\epsilon_g = 2r^2 \left[\left(\frac{\chi}{2r^2} \right)^{\frac{2}{3}} - 1 \right]^{\frac{3}{2}}. \quad (36)$$

VIII. TRANSITION: LANDAU ACTION

Let us turn to the PUT description. Near a PUT, the Green's functions nodes of a general structure are all close to one of the points $(0, \pm 1, 0)$. These two groups of nodes are connected by one or several connectors. Clearly, the phase drop at these connectors is almost π . The action can be expanded in a quadratic form with respect to the deviations of the Green's functions $g_1^i, g_2^i \equiv x_i, z_i$ from this point. If all eigenvalues of this quadratic form are positive, the minimum is achieved at $x_i, z_i = 0$ corresponding to the unprotected situation. If at least one of the eigenvalues is negative, the action minimum is achieved at nonzero x_i, z_i signaling formation of the gapless phase and topological protection. Therefore, a PUT corresponds to an eigenvalue crossing 0. In the spirit of Landau theory of the second-order phase transitions, we keep in the action the corresponding eigenmode only. We denote

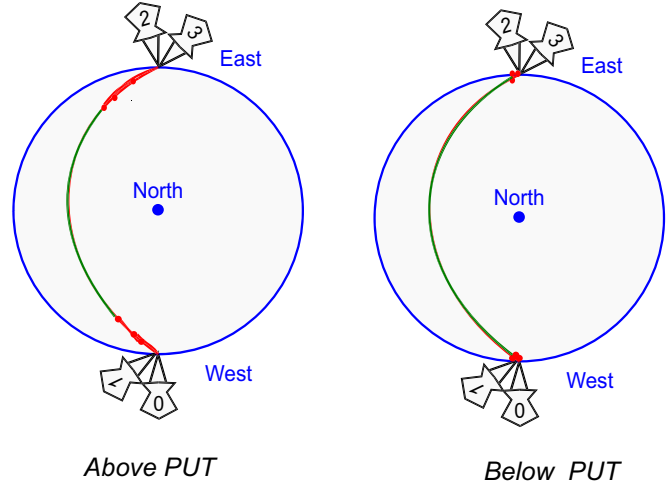


FIG. 6. The Green's functions of the system near a PUT. Precisely in the special point, the network is spanned along one of the big circles. Above the PUT, in the protected phase, the network nodes are at small but finite distances from the west and east poles while a critical connector is spanned between the poles. Above the PUT, in the unprotected phase, the network nodes are precisely in the poles. This results in a gapped phase.

the deviations of this mode x, z . Above the PUT, the nodes are kept at small but finite distances from $(0, \pm 1, 0)$ points. Below the PUT, $x, z = 0$ and all the nodes are in one of these two positions (see Fig. 6).

Taking into account the rotational symmetry at the special point, fourth-order terms in x, z and the anisotropies arising when the superconducting phases of the terminals deviate from the point, we end up with the following action (see Sec. IX for the details of the derivation):

$$S/G_L = \frac{a}{2} (x^2 + z^2) + \frac{b}{4} (x^2 + z^2)^4 - \chi x - \epsilon z - r^2 z^2. \quad (37)$$

Here, a depends on the junction design and is the critical parameter that is negative for protected situation and zero at the PUT. In distinction from a common Landau action, the action (37) defines two complementary order parameters for gapless and gapped phases. The DOS in the gapless phase is proportional to z at $\epsilon = 0$ determined from the action minimization, while the determination of gap ϵ_g requires the extra bifurcation condition $\partial_{xx} S \partial_{zz} S - (\partial_{xz} S)^2 = 0$.

As usual, the action can be rescaled to convenient variables at a given value of a , either positive or negative,

$$\frac{Sb}{G_L a^2} = \pm \frac{\tilde{x}^2 + \tilde{z}^2}{2} + \frac{(\tilde{x}^2 + \tilde{z}^2)^4}{4} - \tilde{\chi} \tilde{x} - \tilde{\epsilon} \tilde{z} - \tilde{r}^2 \tilde{z}^2, \quad (38)$$

where $\tilde{x}, \tilde{z} = x, z \sqrt{b/a^3}$, $\tilde{\chi}, \tilde{\epsilon} = \sqrt{b/a^3} \chi, \epsilon$, and $\tilde{r} = r/\sqrt{a}$. In Figs. 7 and 8 we illustrate the profiles of the DOS and the gap in unprotected and protected regimes close to the PUT, respectively. We make use of the rescaled variables. We see that in the unprotected regime the distinct topological phases touch each other at $\chi = 0$ and $\tilde{r} < 1/\sqrt{2}$. The separating

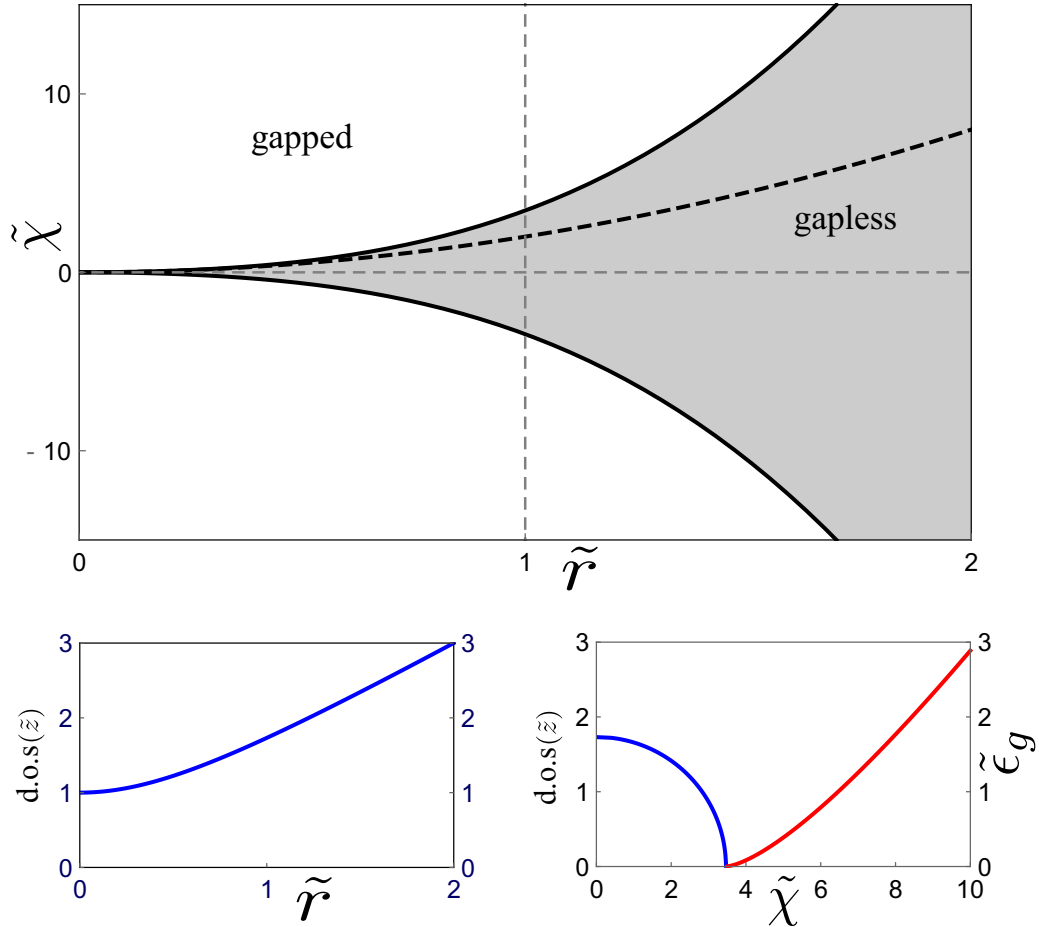


FIG. 7. The situation in the vicinity of a PUT, from the protected side of the transition. We use rescaled variables as defined in Eq. (38). Upper: the domains of gapped and gapless states in the $\tilde{\chi}$ - \tilde{r} plane. Dashed curve gives the asymptotic of the domain boundary in the deep protection regime $\tilde{\chi}, \tilde{r} \ll 1$. Lower: The plots of the gap and DOS along the horizontal (left) and the vertical (right) dashed lines in the upper figure.

gapless phase always persists in the protected regime. At $\tilde{\chi}, \tilde{r} \ll 1$ the action is reduced to that in the deep protection regime [Eq. (10)] giving $\tilde{\chi}_c = 2\tilde{r}^2$. This asymptotic is plotted in Fig. 4(a) with the dashed curve.

Simple analytical formulas are obtained for the boundary between the gapped and gapless states, $\chi_c = 2\tilde{r}^2\sqrt{2\tilde{r}^2 \pm 1}$, and for the gap at $\chi = 0$,

$$\epsilon_g = \frac{2}{3^{\frac{3}{2}}} (1 - 2r^2)^{\frac{3}{2}}. \quad (39)$$

IX. NEAR A PUT: DERIVATION

Let us derive a simple phenomenological model valid for the regime close to a protected–unprotected transition. Here, we use the 3D Cartesian coordinates for both the terminals of the nodes:

$$\vec{g}_a = \frac{1}{\sqrt{1 + \epsilon^2}} (-\zeta_a \sin \chi_a, \zeta_a \cos \chi_a, \epsilon), \quad (40)$$

$$\vec{g}_i = (x_i, \zeta_i \sqrt{1 - s_i^2}, z_i). \quad (41)$$

Here, $s_i^2 = x_i^2 + z_i^2$. Expanding the action around the poles, we have

$$\delta S = \sum_{i,j} \frac{\partial S}{\partial p_{i,j}} \delta p_{i,j} + \sum_{i,a} \frac{\partial S}{\partial p_{i,a}} \delta p_{i,a}. \quad (42)$$

For convenience, let $A_{a,b} = \frac{\partial S}{\partial p_{a,b}}$, $B_{a,b} = \frac{\partial^2 S}{\partial p_{a,b}^2}$. When all the terminals sit at the poles, i.e., $\chi_a = 0$, $\epsilon = 0$, the leading terms in the action are on the second order in x_i and z_i :

$$\delta S \simeq \sum_{i,j} A_{i,j} \left[x_i x_j + z_i z_j - \frac{1}{2} \zeta_i \zeta_j (s_i^2 + s_j^2) \right] - \frac{1}{2} \sum_{i,a} A_{i,a} s_i^2. \quad (43)$$

This expression can be written in matrix form as

$$\delta S \simeq (x_i \ z_i) \begin{pmatrix} \hat{K} & \\ & \hat{K} \end{pmatrix} \begin{pmatrix} x_i \\ z_i \end{pmatrix}, \quad (44)$$

where \hat{K} is a symmetric matrix. The sign of eigenvalues of \hat{K} indicates the stability of the nodes near the poles: when all eigenvalues are positive, all the nodes are kept at the poles for minimum action. In other words, when $\chi_a = 0$, $\epsilon = 0$, a phase transition occurs when one eigenvalue crosses 0 and

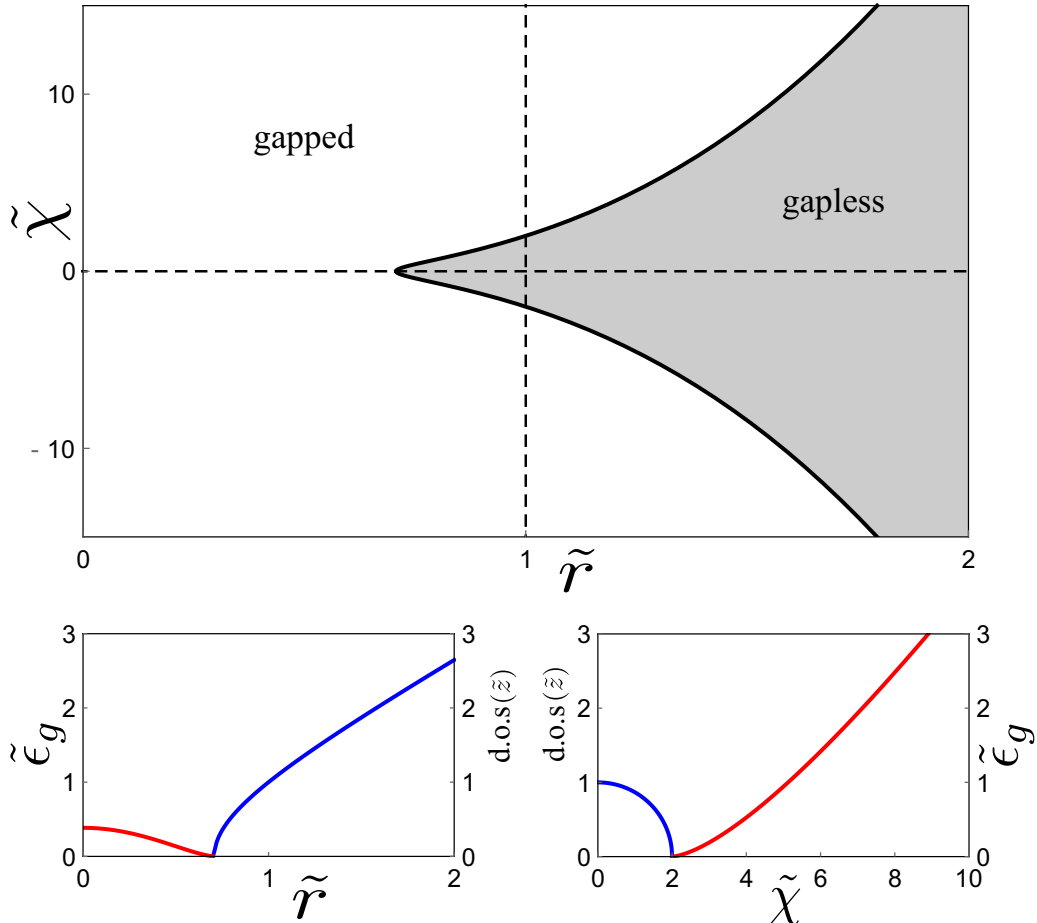


FIG. 8. The situation in the vicinity of a PUT, from the unprotected side of the transition. We make use of the rescaled variables as defined in Eq. (38). Upper: the domains of gapped and gapless states in the $\tilde{\chi}$ - \tilde{r} plane. Lower: The plots of the gap and DOS along the horizontal (left) and the vertical (right) dashed lines in the upper figure.

becomes negative. Let λ_i be the eigenvalues of \hat{K} and u_i and v_i the eigenvectors in x and z subspaces. Then,

$$\delta S = \sum_i \lambda_i (u_i^2 + v_i^2). \quad (45)$$

Let the linear transformation connecting x_i, z_i and u_i, v_i be represented by matrix α , so that

$$\begin{pmatrix} x_i \\ z_i \end{pmatrix} = \begin{pmatrix} \hat{\alpha} & \\ & \hat{\alpha} \end{pmatrix} \begin{pmatrix} u_i \\ v_i \end{pmatrix} \quad (46)$$

or, more explicitly,

$$x_i = \alpha_{i,1} u_1 + \alpha_{i,2} u_2 + \dots, \quad (47)$$

$$z_i = \alpha_{i,1} v_1 + \alpha_{i,2} v_2 + \dots. \quad (48)$$

Let λ_1 be the critical eigenvalue, such that $|\lambda_1| \sim 0 \ll \lambda_{i>1}$. The fluctuation in $u_{i>1}$ and $v_{i>1}$ will be greatly suppressed. In the following, we treat them as effectively equal to 0, i.e., that $x_i \simeq \alpha_{i,1} u_1$, $z_i \simeq \alpha_{i,1} v_1$. Therefore, the quadratic order terms will be approximated by

$$\lambda_1 (u_1^2 + v_1^2). \quad (49)$$

We then collect terms in δS that are lowest order in their respective categories. For coupling between the terminals and

nodes,

$$\begin{aligned} & \sum_{i,a} A_{i,a} (-\zeta_{i,a} \chi_a x_i + \epsilon z_i) \\ & \simeq - \sum_{i,a} A_{i,a} \zeta_{i,a} \chi_a \alpha_{i,1} u_1 + \sum_{i,a} A_{i,a} \alpha_{i,1} \epsilon v_1. \end{aligned} \quad (50)$$

Let

$$\chi' = - \sum_{i,a} A_{i,a} \zeta_{i,a} \chi_a \alpha_{i,1}, \quad \epsilon' = \sum_{i,a} A_{i,a} \alpha_{i,1} \epsilon \quad (51)$$

and replacing u_1 and v_1 with x and z , we have

$$\sum_{i,a} A_{i,a} (-\zeta_{i,a} \chi_a x_i + \epsilon z_i) = \chi' x + \epsilon' z. \quad (52)$$

Other terms will be treated in a similar fashion. To ensure that the action has a lower bound, it is necessary to include terms fourth order in x and z . For other terms, we proceed in a way similar to how terms in the deep protection case were treated: only first-order terms and second-order terms that do not vanish when first terms vanish are retained. The final result is a simple Ginzburg-Landau-type action

$$\delta S = \frac{a}{2} (x^2 + z^2) + \frac{b}{4} (x^2 + z^2)^2 + \chi' x + \epsilon' z - r^2 z^2, \quad (53)$$

where

$$a = 2\lambda_1, \quad (54)$$

$$\begin{aligned} b &= -\frac{1}{8} \sum_{i,j} A_{i,j} \zeta_i \zeta_j (\alpha_{i,1}^4 + \alpha_{j,1}^4 - 2\alpha_{i,1}^2 \alpha_{j,1}^2) \\ &+ \sum_{i,j} B_{i,j} \left[\alpha_{i,1} \alpha_{j,1} - \frac{1}{2} \zeta_i \zeta_j (\alpha_{i,1}^2 + \alpha_{j,1}^2) \right] + \frac{1}{4} \sum_{i,a} B_{i,a} \alpha_{i,1}^4, \\ r^2 &= \sum_{i,a} B_{i,a} \chi_a^2 \alpha_{i,a}^2. \end{aligned} \quad (55)$$

To have a dimensionless action such that we can make direct comparison with the deep protection regime case, divide the action by $\sum_{i,a} A_{i,a} \alpha_{i,1}$,

$$\delta \tilde{S} = \frac{\bar{a}}{2} (x^2 + z^2) + \frac{\bar{b}}{4} (x^2 + z^2)^2 + \bar{\chi} x + \epsilon z - \bar{r}^2 z^2 \quad (56)$$

with $\bar{a}, \bar{b}, \bar{\chi}, \bar{r}^2 = a, b, \chi', r^2 / \sum_{i,a} A_{i,a} \alpha_{i,1}$. We rescale the action such that the coefficient for the quadratic and fourth-order terms become 1:

$$\delta \tilde{S} = \frac{1}{2} (\tilde{x}^2 + \tilde{z}^2) + \frac{1}{4} (\tilde{x}^2 + \tilde{z}^2)^2 + \tilde{\chi} \tilde{x} + \tilde{\epsilon} \tilde{z} - \tilde{r}^2 \tilde{z}^2, \quad (57)$$

where $\tilde{S} = \bar{S} b / a^2$, $\tilde{x}, \tilde{z} = x, z \sqrt{b/a}$, $\tilde{\chi}, \tilde{\epsilon} = \sqrt{b/a^3} \chi, \epsilon$, and $\tilde{r} = r / \sqrt{a}$. The phase boundary, as well as gap and DOS in gapped and gapless phases can be found in an identical way as in the previous section. However, simple analytical expressions are not available except to the phase boundary

$$\chi_c = \begin{cases} 2r^2 \sqrt{2r^2 - 1}, & a > 0 \\ 2r^2 \sqrt{2r^2 + 1}, & a < 0 \end{cases} \quad (58)$$

and the gap when $\chi = 0$ in the $a > 0$ case

$$\epsilon_g = \frac{2}{3^{\frac{3}{2}}} (1 - 2r^2)^{\frac{3}{2}}. \quad (59)$$

-
- [1] N. D. Mermin, *Rev. Mod. Phys.* **51**, 591 (1979).
- [2] M. Z. Hasan and C. L. Kane, *Rev. Mod. Phys.* **82**, 3045 (2010).
- [3] X.-L. Qi and S.-C. Zhang, *Rev. Mod. Phys.* **83**, 1057 (2011).
- [4] X. Wan, A. M. Turner, A. Vishwanath, and S. Y. Savrasov, *Phys. Rev. B* **83**, 205101 (2011).
- [5] M. König, S. Wiedmann, C. Brüne, A. Roth, H. Buhmann, L. W. Molenkamp, X.-L. Qi, and S.-C. Zhang, *Science* **318**, 766 (2007).
- [6] D. Hsieh, Y. Xia, D. Qian, L. Wray, F. Meier, J. H. Dil, J. Osterwalder, L. Patthey, A. V. Fedorov, H. Lin, A. Bansil, D. Grauer, Y. S. Hor, R. J. Cava, and M. Z. Hasan, *Phys. Rev. Lett.* **103**, 146401 (2009).
- [7] X. Yang, I. Miotkowski, C. Liu, J. Tian, N. Hyoungdo, N. Alidoust, H. Jiuning, C.-K. Shih, M. Zahid Hasan, and Y. P. Chen, *Nat. Phys.* **10**, 956 (2014).
- [8] A. Y. Kitaev, *Phys.-Usp.* **44**, 131 (2001).
- [9] L. Fu and C. L. Kane, *Phys. Rev. B* **79**, 161408(R) (2009).
- [10] V. Mourik, K. Zuo, S. M. Frolov, S. R. Plissard, E. P. A. M. Bakkers, and L. P. Kouwenhoven, *Science* **336**, 1003 (2012).
- [11] S. Nadj-Perge, I. K. Drozdov, J. Li, H. Chen, S. Jeon, J. Seo, A. H. MacDonald, B. A. Bernevig, and A. Yazdani, *Science* **346**, 602 (2014).
- [12] R. Riwar, M. Houzet, J. Meyer, and Y. V. Nazarov, *Nat. Commun.* **7**, 1167 (2016).
- [13] E. Eriksson, R.-P. Riwar, M. Houzet, J. S. Meyer, and Y. V. Nazarov, *Phys. Rev. B* **95**, 075417 (2017).
- [14] T. Yokoyama and Y. V. Nazarov, *Phys. Rev. B* **92**, 155437 (2015).
- [15] T. Yokoyama, J. Reutlinger, W. Belzig, and Y. V. Nazarov, *Phys. Rev. B* **95**, 045411 (2017).
- [16] E. Strambini, S. D'Ambrosio, F. Vischi, F. S. Bergeret, Y. V. Nazarov, and F. Giazotto, *Nat. Nanotechnol.* **11**, 1055 (2016).
- [17] M. Amundsen, J. A. Ouassou, and J. Linder, *Sci. Rep.* **7**, 40578 (2017).
- [18] A. I. Larkin and Yu. N. Ovchinnikov, *Zh. Eksp. Teor. Fiz.* **55**, 2262 (1968) [*Sov. Phys. JETP* **28**, 1200 (1969)].
- [19] W. Belzig, F. K. Wilhelm, C. Bruder, G. Schön, and A. D. Zaikin, *Superlattices Microstruct.* **25**, 1251 (1999).
- [20] Y. V. Nazarov and Y. M. Blanter, *Quantum Transport: Introduction to Nanoscience* (Cambridge University Press, Cambridge, 2009).

We numerically computed the gap and DOS in general and the result is presented in the previous section.

X. CONCLUSIONS

In conclusion, we have studied the topological projection of distinct gapped states in N -terminal superconducting junction. The protection is manifested as a gapless state separating the gapped states in the parameter space of $N - 1$ superconducting phases. We reveal that the protection may cease near special points as a result of a protection–unprotection transition in the parameter space of the junction designs. We have found a Landau action that describes the the vicinity of the transition. In distinction from common Landau actions, this one permits evaluation of complementary order parameters, DOS and gap, for gapless and gapped states.

We speculate that the known generality of Landau actions would permit to extend our approach to a wider variety of topological phenomena in condensed matter physics. Such phenomena may include the gapping of the edge modes at the interfaces of distinct topological insulators that separate gapped states in real rather than parametric space. While the concrete physical mechanisms responsible for such PUTs may be involved and unknown, the essential phenomenology of the transition may be captured by a Landau action in a form proposed in this paper.

ACKNOWLEDGMENTS

This work is part of the research programme of the Foundation for Fundamental Research on Matter (FOM), which is part of the Netherlands Organisation for Scientific Research (NWO). The authors acknowledge useful discussions with A. Akhmerov.

- [21] M. Tinkham, *Introduction to Superconductivity: Second Edition*, Dover Books on Physics (Dover, New York, 2004).
- [22] L. D. Landau, Zh. Eksp. Teor. Fiz. **7**, 19 (1937) [Ukr. J. Phys. **53**, 25 (2008)].
- [23] J. C. Tolédano and P. Tolédano, *The Landau Theory of Phase Transitions* (World Scientific, Singapore, 1987), <https://www.worldscientific.com/doi/pdf/10.1142/0215>.
- [24] X. Chen, Z.-C. Gu, and X.-G. Wen, Phys. Rev. B **83**, 035107 (2011).
- [25] L. Tsui, H.-C. Jiang, Y.-M. Lu, and D.-H. Lee, Nucl. Phys. B **896**, 330 (2015).
- [26] C. Padurariu, T. Jonckheere, J. Rech, R. Mélin, D. Feinberg, T. Martin, and Y. V. Nazarov, Phys. Rev. B **92**, 205409 (2015).
- [27] C. W. J. Beenakker, Rev. Mod. Phys. **69**, 731 (1997).
- [28] Y. V. Nazarov, Phys. Rev. Lett. **73**, 134 (1994).